Phys. Lett. B 850 (2024) 138522

Contents lists available at ScienceDirect

Physics Letters B

journal homepage: www.elsevier.com/locate/physletb

Letter

Formation mechanism of decay fragments in spontaneous ternary fission of heavy nuclei

Sh.A. Kalandarov [a], R.B. Tashkhodjaev [b,c,d,*], O.K. Ganiev [e,f]

[a] Joint Institute for Nuclear Research, 141980 Dubna, Russia
[b] New Uzbekistan University, Movarounnahr street 1, 100000, Tashkent, Uzbekistan
[c] Central Asian University, Milliy Bog' Street 264, 111221, Tashkent, Uzbekistan
[d] Inha University In Tashkent, Ziyolilar 9, 100170, Tashkent, Uzbekistan
[e] Institute of Nuclear Physics, Ulugbek, 100214, Tashkent, Uzbekistan
[f] National University of Uzbekistan, 100174, Tashkent, Uzbekistan

ARTICLE INFO

Editor: B. Balantekin

ABSTRACT

A model for describing spontaneous ternary fission of heavy nuclei is presented. It follows from the suggested model that heavy nuclei have the same half-lives in spontaneous ternary and binary fission processes. The collinear cluster tripartition process observed in FOBOS experiments is found to be the dominant reaction channel in spontaneous true ternary fission of heavy nuclei within our model. Competition between binary fission and the formation of a trinuclear system, which is responsible for the ratio of spontaneous ternary and binary fission yields, is introduced.

1. Introduction

The process of nuclear decay began to be intensively studied in the first half of the last century. Early theoretical models for alpha decay by Gamow [1] and binary fission by Bohr and Wheeler [2] were developed. Interest in ternary fission of heavy nuclei arose soon after the discovery of binary fission [3–5]. First theoretical models of the ternary fission were developed in the framework of the liquid drop model [6]. Later, in 1980s, the ternary fission process with emitting alpha-particles or other light nuclei (Li, Be, etc) was investigated by a number of nuclear scientists [7–10]. Three types of ternary fission of heavy nuclei have been observed: splitting into three fragments of nearly equal masses (symmetric tripartition or true ternary fission), fission with the lightest fragment in the mass range $A > 30$ (asymmetric tripartition), and fission with emitting light charged particle, mainly α particle, as a third fragment (charged particle accompanied fission). These three types of ternary decay, although being energetically favored compared to binary fission, were found to be extremely rare with the measured upper limit yields 2×10^{-9}, 8×10^{-8} and 3×10^{-3}, respectively, relative to binary fission [9].

Later, a series of experiments, carried out by the FOBOS group at the Flerov Laboratory of Nuclear Reactions, JINR on ternary fission of heavy nuclei raised new interest to the ternary decay process [11–15]. In those experiments, the existence of a new type of ternary decay in the reaction ^{235}U(n$_{th}$,f) and ^{252}Cf(sf), namely collinear cluster tri-partition (CCT), was reported. The measured yield of the CCT process turned out to be surprisingly high, 4×10^{-3} per binary fission [12]. The collinear configuration of the ternary system and the high experimental yield of CCT products was explained by assuming that collective motion through hyper-deformed pre-scission shapes of the mother nucleus leads to a linear arrangement of three clusters due to the lowest Coulomb potential energy. Moreover, the Q-values of ternary fission are 25–30 MeV more positive than for binary fission due to the formation of magic nuclei. These experimental results invoke a large number of theoretical investigations of the CCT process [16–29]. Although many experimental features of the CCT process were well described in these theoretical works, the mechanism of formation of a collinear ternary system, which is responsible for high CCT yields in FOBOS experiments, is still unclear. Since the first experimental evidence of ternary fission comes from α particle accompanied fission [9] of heavy nuclei, the mechanism for the formation of a trinuclear configuration is assumed to be as in Fig. 1 of Ref. [30]. In the fission process of heavy nuclei, during dynamical motion from saddle to scission points, the third fragment can indeed be formed in the neck region before the rupture of the neck. Since this process takes place dynamically and future fission fragments are in the opposite motion, the probability of formation of clusters in

* Corresponding author.
E-mail address: tashkhodjaev@yahoo.com (R.B. Tashkhodjaev).

https://doi.org/10.1016/j.physletb.2024.138522
Received 1 December 2023; Received in revised form 5 February 2024; Accepted 5 February 2024
Available online 7 February 2024

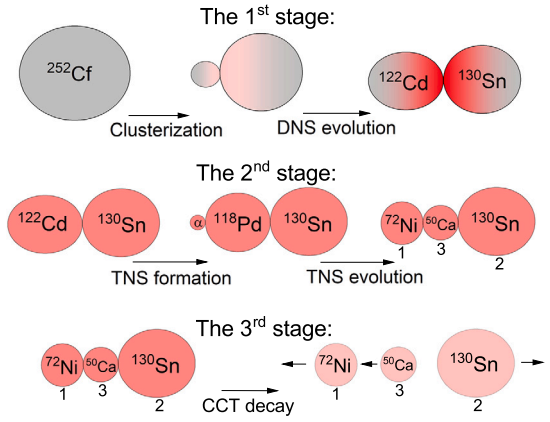

Fig. 1. Mechanism of formation of CCT fragments.

the neck region decreases with increasing size of a cluster, which explains relatively high yield of α particle accompanied fission. However, this scenario of ternary fission, in our opinion, can not explain the high yields of the CCT process with a relatively large size ($A \sim 50$) of a middle nucleus.

In our recent works [28,31], we have shown that the decay time of a trinuclear system (TNS) after the formation of TNS is $\sim 10^{-20}$ s. This means that the half-life time of ^{252}Cf in spontaneous ternary decay is determined by the time of formation of TNS. So both the yield and the half-life time in spontaneous ternary fission of ^{252}Cf are mainly determined at the TNS formation stage. Hence, we conclude that for any theoretical model of ternary fission, the formation mechanism of a trinuclear configuration is expected to be decisive for describing experimental data and predicting new features of the process. Thus, the motivation of the present work is to reveal the formation mechanism of TNS in spontaneous ternary fission of heavy nuclei. Here we consider the formation of TNS as a subsequent formation of dinuclear systems. The nucleon transfer process between TNS nuclei is responsible for the formation of different trinuclear systems by analogy with the dinuclear system (DNS) model [32–35], which is widely applied to describe fusion-fission reactions and spontaneous fission processes [36–38].

This paper is organized as follows: in Sec. 2, the concepts of our model to describe spontaneous ternary fission is presented. In Sec. 3, the details of calculations of potential energies for DNS and TNS are provided. The results of application of the model for describing spontaneous ternary fission of ^{252}Cf are presented in section 4. In Sec. 5, summary and conclusions are given.

2. Concept of formation of trinuclear system in spontaneous ternary fission of heavy nuclei

In our model, spontaneous ternary fission of heavy nuclei takes place in three consecutive stages (Fig. 1): first, the formation of asymmetric DNS and its evolution in mass (and charge) asymmetry coordinates towards symmetric DNS configurations, then the transformation of one of the nearly symmetric DNS nuclei into another DNS, thus forming the TNS, and finally the decay of TNS into three fragments. In the following, we consider each of these stages in more detail.

In the first stage, a mononucleus transforms into an asymmetric DNS due to the spontaneous condensation of valence nucleons to a light cluster nucleus. The experimentally observed cluster radioactivity of radium isotopes and actinides gives a cue that clusterization of valence nucleons above the Pb core is peculiar to all elements heavier than Pb. However, for heavy isotopes of uranium and transuranium elements it is impossible for all valence nucleons to be condensed to a cluster. This would be energetically unfavorable as it would lead to the formation of light super neutron-rich nuclei with a very low binding energy of neutrons. As a consequence, part of the nucleons will be found in covalent states, i.e. they will envelop in their motion both the cluster nucleus and the associated heavy nucleus. These covalent nucleons play an important role in the evolution of the dinuclear molecule. They encompass in their motion both nuclei of the nuclear molecule, intensify their interaction, and enhance the transfer of kinetic energy of the relative motion into the excitation energy [39,40]. It is also known that the number of valence nucleons outside the major shell (a level with a magic number) play an important role in heavy ion fusion reactions, too [41,42]. For more information about nuclear clusters and molecules, we refer readers to invaluable books edited by W. Greiner [43] and by C. Beck [44–46].

As a result of nucleon condensation, different light cluster nuclei, e.g., α particle, ^{8,9}Be and ^{12,14}C can be formed on the surface of a heavy nucleus leading to the formation of an asymmetric DNS. The asymmetric DNS then evolves in two competing coordinates: relative distance coordinate R between the centers of heavy nuclei and a cluster, and mass/charge asymmetry coordinates (due to the nucleon exchange). The motion in R of asymmetric DNS is responsible for the cluster radioactivity. The nucleon exchange process between nuclei in DNS leads to the evolution of asymmetric DNS towards more symmetric configurations in accordance with potential energy of DNS. This first stage ends up with the formation of excited and energetically favorable symmetric DNS configurations (see Fig. 1). It is worth noting that motion in the R coordinate of symmetric DNS leads to spontaneous binary fission. Since the decay of symmetric DNS takes place from excited DNS states, this first stage (clusterization + motion towards symmetric DNS) mainly determines the half-lives for spontaneous fission [36]. The fully quantum mechanical description of the nucleon clusterization process is a quite complex task, and cluster formation probabilities can be calculated with using different approximations, for example, within the approach given in Ref. [36].

In the second stage, one of the excited nuclei in symmetric DNS transforms into another asymmetric DNS, leading to the formation of TNS. Here we assume that the light cluster in TNS appears on the outer side of the heavier nucleus. Indeed, the Pauli principle and strong nuclear forces will prevent the formation of a light cluster between the two heavy nuclei in DNS. The TNS formation process competes with the binary fission of excited symmetric DNS, which takes place in a nuclear time scale. The nucleon transfer between nuclei in TNS leads to the formation of TNS configurations with different asymmetries. One should note that due to the Coulomb forces the nuclei in TNS are collinearly placed, which favors the CCT mode of ternary fission observed in the FOBOS experiments [12].

In the third stage, excited TNS decays into three fragments. The dynamics of TNS decay in the presence of microscopic friction forces was investigated in our previous work [28].

As a summary of this section, we conclude that since the second and third stages of spontaneous ternary fission take place in nuclear times under the influence of excitation energy, the first (clusterization + motion towards symmetric DNS) stage determines the half-life time of spontaneous ternary fission. It implies that within the suggested model, spontaneous binary and ternary fission have almost the same half-lives. The ratio of ternary to binary fission is determined in the second stage; from the competition between the decay of symmetric DNS and TNS formation processes.

3. Potential energies of DNS and TNS

The potential energy $U_{\rm DNS}$ of a dinuclear system is calculated as

$$U_{\rm DNS} = V_{int,\rm DNS} + Q_{\rm DNS}, \quad (1)$$

where $Q_{\rm DNS} = B_i + B_j - B_{\rm CN}$, B_i, B_j and $B_{\rm CN}$ are mass excesses of two nuclei forming the DNS and a compound nucleus (CN), respectively. Here "i" and "j" denote the nuclei in the DNS. Experimental values of mass excesses by Audi et al. [47] are used in the current work. The total interaction potential $V_{int,\rm DNS}$ of the DNS is the sum of the nuclear

V_N and Coulomb potential V_C energies. For the calculation of Coulomb interaction between nuclei in the DNS we use the Wong formula [48]:

$$V_{Cij}(R_{ij}, Z_i, Z_j) = \frac{Z_i Z_j e^2}{R_{ij}} + \frac{Z_i Z_j e^2}{R_{ij}^3}\sqrt{\frac{9}{20\pi}}(R_{0i}^2\beta_i + \\ + R_{0j}^2\beta_j) + \frac{Z_i Z_j e^2}{R_{ij}^3}\frac{3}{7\pi}\left(R_{0i}^2\beta_i^2 + R_{0j}^2\beta_j^2\right). \quad (2)$$

Here, β_i and β_j are the quadrupole deformation parameters, R_{0i} and R_{0j} are the radii of spherical nuclei, R_{ij} is the relative distance between their centers, and Z_i and Z_j are their charge numbers. The nuclear part of the interaction is calculated using the double folding formalism with the density dependent effective nucleon-nucleon forces f_{eff} by Migdal [49]

$$V_{Nij}(R_{ij}) = \int \rho_i(\mathbf{r}) f_{\text{eff}}(\mathbf{r}, \mathbf{R}_{ij}) \rho_j(\mathbf{r} - \mathbf{R}_{ij}) d\mathbf{r}, \quad (3)$$

where $f_{\text{eff}}(\mathbf{r}, \mathbf{R}_{ij}) = C_0\left[F_{\text{in}} + (F_{\text{ex}} - F_{\text{in}})\frac{\rho_0 - \rho(\mathbf{r}, \mathbf{R}_{ij})}{\rho_0}\right]$, and $\rho(\mathbf{r}, \mathbf{R}_{ij}) = \rho_i(\mathbf{r}) + \rho_j(\mathbf{r} - \mathbf{R}_{ij})$. The following set of constants is used for the Migdal forces [49]: $C_0 = 300$ MeV·fm^3, $F_{\text{ex,in}} = f_{\text{ex,in}} + f'_{\text{ex,in}}\frac{(A_i - 2Z_i)(A_j - 2Z_j)}{(A_i + 2Z_i)(A_j + 2Z_j)}$, $f_{in} = 0.09$, $f_{\text{ex}} = -2.59$, $f'_{in} = 0.42$ and $f'_{\text{ex}} = 0.54$. The nuclear densities are taken in the form of two-parameter Fermi distribution:

$$\rho_i(\mathbf{r}) = \frac{\rho_0}{1 + \exp\left(\frac{r - R_i(\theta_i)}{a_0}\right)}, \quad (4)$$

where $\rho_0 = 0.17$ fm^{-3} is the nuclear density at the center of a nucleus, a_0 is the diffuseness parameter, and $R_i(\theta_i) = r_0 A_i^{1/3}(1 + \beta_i Y_{20}(\cos\theta_i))$ is the radius of a deformed nucleus. Here, r_0 is the radius parameter, Y_{20} is the Legendre polynomial and A_i is the mass number. The quadrupole deformation parameters β_i are taken from S. Raman et al. [50] presented for excited 2^+ states. When $\rho(\mathbf{r}, \mathbf{R}_{ij}) > \rho_0$, the nuclear part V_{Nij} becomes repulsive, which reflects the Pauli blocking principle. The DNS is located at the minimum of the interaction potential, which corresponds to $R_{ij} \approx R_i + R_j + 0.5$ fm. Due to the fast nucleon exchange process, N/Z equilibration takes place in DNS [35]. This means that equilibrium masses of DNS nuclei for given charge numbers are determined from the potential energy minimum with respect to A_i and A_j.

The potential energy of a TNS is calculated as

$$U_{\text{TNS}} = V_{int,\text{TNS}} + Q_{\text{TNS}}, \quad (5)$$

where $Q_{\text{TNS}} = B_1 + B_2 + B_3 - B_{CN}$. The interaction potential $V_{int,\text{TNS}}$ for the TNS is calculated as the sum of two body interactions, i.e. $V_{int,\text{TNS}} = V_{int,12} + V_{int,23} + V_{int,13}$. The TNS is located at the minimum of the interaction potential with respect to the relative distance coordinates R_{13} and R_{23}. The masses of fragments for a certain charge number Z is determined from N/Z equilibrium, as mentioned above.

In the DNS model, the radius parameter r_0 and the diffuseness parameter a_0 in the nuclear density formula (4) were fixed to the values $r_0 = 1.17$ fm and $a_0 = 0.54$ fm for the fusion-fission and quasifission reactions [51]. However, in [39,40], Volkov et al. found the values $r_0 = 1.2$ fm and $a_0 = 0.54 + (0.011 \cdot Z)^2(A - 2Z)/A$ fm to be better for describing the processes of thermal neutron induced fission and spontaneous fission of heavy nuclei. This functional form of the diffuseness parameter takes into account its dependence on neutron excess. In fission of heavy nuclei, two interacting nuclei (future fission fragments) at a saddle point are more neutron rich comparing to DNS nuclei formed in fusion reactions. Therefore, in this work, we take values of r_0 and a_0 from Ref. [39,40].

4. Spontaneous ternary fission of ^{252}Cf

In the first stage of spontaneous ternary fission of ^{252}Cf, as a result of clusterization process, light clusters beginning from α particle up to

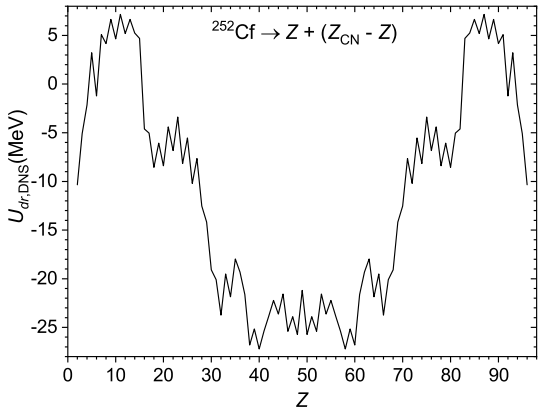

Fig. 2. The calculated driving potential of cluster + heavy nucleus for ^{252}Cf as a function of the charge number Z of one nucleus in the DNS.

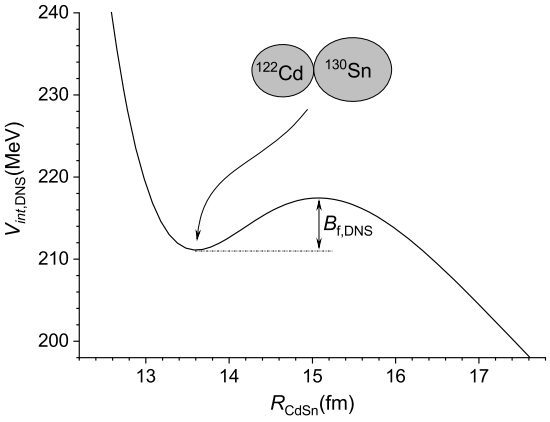

Fig. 3. The dependence of the interaction potential $V_{int,\text{DNS}}$ on the relative distance R_{CdSn} coordinate for ^{122}Cd+ ^{130}Sn.

isotopes of sulfur, which are above the Pb core, can be formed on the surface of the mother nucleus. The calculation of spectroscopic factors for these clusters is out of the aim of the present work. We can refer the readers to Ref. [36], where the method of calculation of cluster formation probabilities is given in the framework of the DNS model for describing cluster radioactivity of heavy nuclei. The driving potential of cluster + heavy nucleus for ^{252}Cf is presented in Fig. 2 as a function of the charge number Z of one nucleus in the DNS. One can see that the formation of light clusters ($Z_{cluster} < 5$) can not lead to the evolution of asymmetric DNS towards symmetric configurations since the nucleon transfer cannot happen to energetically forbidden DNS states with $4 < Z_{cluster} < 16$. Hence, in spontaneous ternary fission of ^{252}Cf, the clustering process leads to the formation of a cluster nucleus S on the surface of the Pb core. The formed asymmetric DNS will evolve by the nucleon transfer process towards more symmetric configurations. It is seen from Fig. 2 that symmetric DNS states can have about 20–30 MeV excitation energy and lighter nuclei in DNS can have a charge number $Z = 30$–48, according to the potential energy of DNS. The formation probabilities of nearly symmetric DNS configurations are proportional to the relevant level densities, which exponentially depend on the corresponding potential energy.

As an example, let us discuss the formation process of TNS from one of the most energetically favorable DNS configuration Cd + Sn. The nearly symmetric DNS state ^{122}Cd+ ^{130}Sn has $E^*_{\text{DNS}} = 25.73$ MeV excitation energy (see Fig. 2). As mentioned above, the DNS is located at the minimum of the interaction potential at relative distances $R_{ij} \approx R_i + R_j + 0.5$ fm and the decay barrier $B_{f,\text{DNS}} = 6.34$ MeV prevents it from splitting (Fig. 3). Under the influence of the excitation energy, an α particle can be formed on the outer surface of Cd, thus

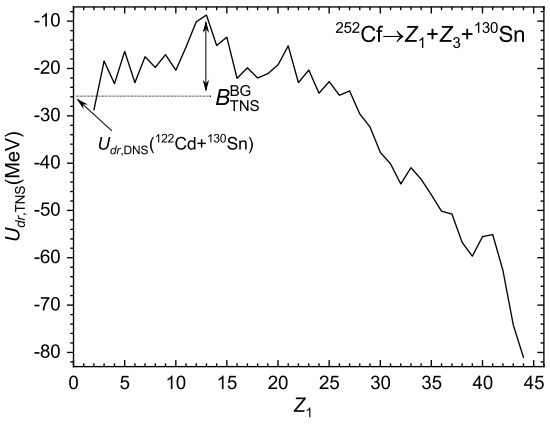

Fig. 4. The driving potential of TNS formed from a nearly symmetric DNS state ^{122}Cd+ ^{130}Sn, as a function of the left border nucleus charge number Z_1.

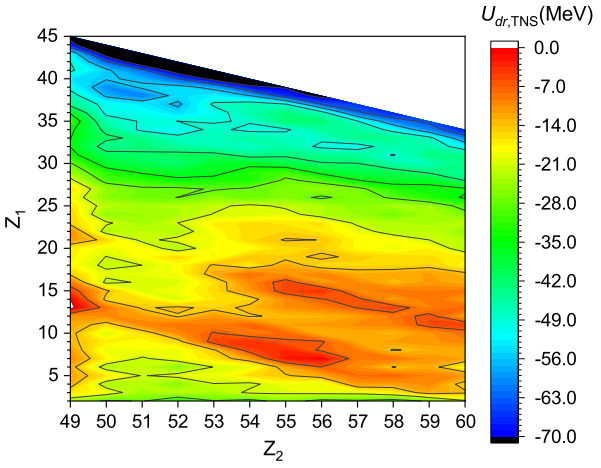

Fig. 5. The driving potential of TNS $U_{dr,TNS}$ formed from nearly symmetric DNS configurations as a function of the charge number Z_1 and Z_2 of border nuclei.

forming the TNS. Further TNS evolution by nucleon transfer between fragments leads to the formation of more symmetric configurations, as illustrated schematically in Fig. 1. One should note that since Sn is a magic nucleus, the nucleon exchange process during the evolution of TNS does not alter the border nucleus 2, which remains to be Sn. The driving potential of the TNS as a function of the left border nucleus charge number Z_1 is presented in Fig. 4 for TNS formed from a nearly symmetric DNS state ^{122}Cd+ ^{130}Sn. To reach more symmetric TNS configurations, the system should pass through the potential barrier, which is defined by the height of the Businaro-Gallone (B.G.) point B^{BG}_{TNS} shown in Fig. 4. The value of the potential barrier obtained with respect to the energy of the ^{122}Cd+ ^{130}Sn configuration is $B^{BG}_{TNS} = 17.01$ MeV. As already mentioned, the TNS formation process competes with the binary decay of the ^{122}Cd+ ^{130}Sn DNS configuration. This competition mainly determines the ratio of ternary to binary fission yields. One can estimate this ratio by the approximated formula:

$$\frac{Y_{ter.fiss.}}{Y_{bin.fiss.}} \approx \exp[-(B^{BG}_{TNS} - B_{f,DNS})/T_{DNS}], \quad (6)$$

where T_{DNS} is the temperature of the ^{122}Cd+ ^{130}Sn DNS configuration. The temperature can be calculated with the Fermi-gas model formula as: $T_{DNS} = \sqrt{E^*_{DNS}/a}$ with the level density parameter $a = A_{CN}/12$. This estimation gives the result $Y_{ter.fiss.}/Y_{bin.fiss.} = 6.7 \times 10^{-5}$, which is very close to the CCT yields observed in FOBOS experiments [15].

After passing the B.G. point, TNS quickly reaches more symmetric configurations as potential energy decreases, so the size of the left border nucleus 1 increases. One can see from Fig. 4 that the potential energy of the ternary system drastically decreases as the size of the middle nucleus decreases, reaching -80 MeV for the case where the middle nucleus is Be. This reduction of the potential energy of a ternary system can transform to either inner excitation energies or kinetic energies of border nuclei. This leads to the system becoming quite unstable after passing the B.G. point, and system mostly decays before reaching such configurations where the middle nucleus is one of the lightest cluster nuclei. Thus, the relative yields of ternary decay products are strongly affected by the dynamics of the ternary system in mass asymmetry and relative distance coordinates after passing the B.G. point.

In the general case, TNS can be formed in a similar way from any energetically possible DNS states. The two-dimensional driving potential of TNSs formed from nearly symmetric DNS configurations with $Z_2 = 49$–60 is presented in Fig. 5. One can see that the nucleon exchange process between TNS nuclei favors the formation of TNSs with $Z_2 = 50$–52. This means that the ternary systems $Z_1 + Z_3$ + Xe, $Z_1 + Z_3$ + Ba and $Z_1 + Z_3$ + Ce partially go to the $Z_1 + Z_3$ + Sn and $Z_1 + Z_3$ + Te states due to the nucleon exchange between middle and right border nuclei before passing the B.G. point. This may lead to higher yields

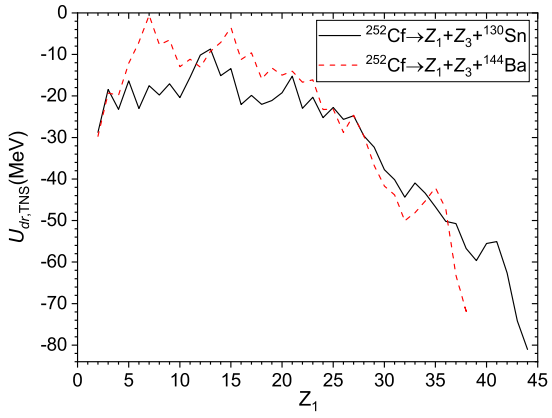

Fig. 6. The driving potential of TNS formed from nearly symmetric DNS states ^{122}Cd+ ^{130}Sn and ^{108}Mo+ ^{144}Ba as a function of the left border nucleus charge number Z_1 for fixed right border nuclei ^{130}Sn (black solid line) and ^{144}Ba (red dashed line).

of the ternary products $Z_1 + Z_3$ + Sn and $Z_1 + Z_3$ + Te in comparison with the ternary products $Z_1 + Z_3$ + Xe, $Z_1 + Z_3$ + Ba and $Z_1 + Z_3$ + Ce [12,15].

For clarity, a comparison of driving potentials of TNSs with fixed right border nuclei (Sn and Ba) is represented in Fig. 6. For the ternary system Z_1 + Z_3 + Ba with the fixed right border nucleus Ba, the ratio $Y_{ter.fiss.}/Y_{bin.fiss.}$, which is calculated by formula (6) is much smaller since the B.G. point is much higher than for Z_1 + Z_3 + Sn. The dependence of $Y_{ter.fiss.}/Y_{bin.fiss.}$ on the fixed charge number Z_2 of the right border nucleus is given in Fig. 7. However, as already mentioned, the nucleon exchange process between TNS nuclei formed from nearly symmetric DNS states with $Z_2 = 49$–60 leads to the formation of TNSs with $Z_2 = 50$–52 before passing the B.G. point (see Fig. 5) with high probability. Therefore, the ratio $Y_{ter.fiss.}/Y_{bin.fiss.}$ for all TNS formed from nearly symmetric DNS states will be close to the value 6.7×10^{-5}, which is obtained for the $Z_1 + Z_3$ + Sn case.

As we have noticed, the relative yields of ternary products depend strongly on the dynamics of the system after passing the B.G. point in mass asymmetry and relative distance coordinates. Obviously, the decay of the ternary systems ^{50}Ca+ ^{72}Ni+ ^{130}Sn and ^{72}Ni+ ^{50}Ca+ ^{130}Sn with magic nuclei Ca, Ni, Sn are best candidates for experimental observation of the CCT process. The calculated excitation energy of the TNS ^{72}Ni+ ^{50}Ca+ ^{130}Sn (^{50}Ca+ ^{72}Ni+ ^{130}Sn), which is defined as the potential energy of TNS with respect to the energy of ^{252}Cf, is 29.61 MeV (19.25 MeV). The TNS ^{72}Ni+ ^{50}Ca+ ^{130}Sn is located at the minimum of

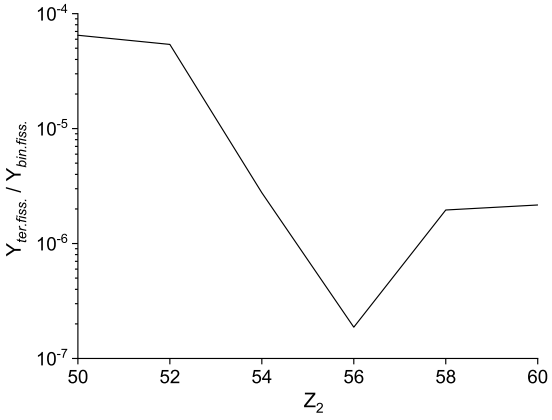

Fig. 7. The dependence of $Y_{ter.fiss.}/Y_{bin.fiss.}$ given by formula (6) on the charge number Z_2 of the right border nucleus in TNS.

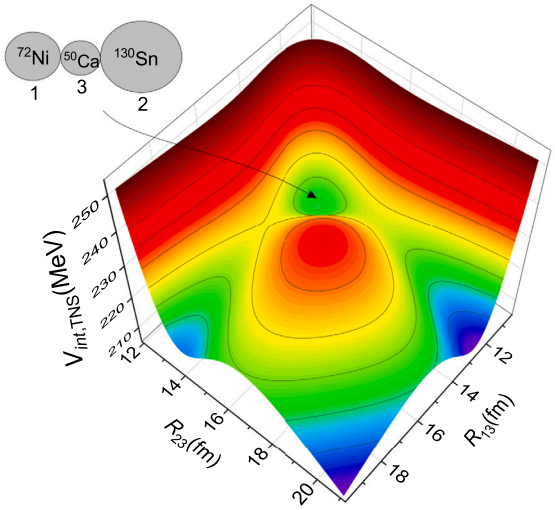

Fig. 8. The total interaction potential $V_{int,\mathrm{TNS}}$ as a function of the relative distances R_{13} and R_{23} for the ^{72}Ni+^{50}Ca+^{130}Sn configuration.

the interaction potential $V_{int,\mathrm{TNS}}$ with respect to the relative distances R_{13} and R_{23}, as shown in Fig. 8. The dynamics of the ternary decay of the TNS ^{72}Ni+^{50}Ca+^{130}Sn is described in our recent work [28]. After the decay, the excited ternary fission fragments can emit neutrons.

5. Summary and conclusions

In this paper, a model to describe a mechanism of spontaneous ternary fission is suggested. According to the model, spontaneous ternary fission of heavy nuclei takes place in three consecutive stages: first, the formation of an asymmetric DNS and its evolution in the mass and charge asymmetry coordinates towards symmetric DNS configurations, second, the transformation of one of the symmetric DNS nuclei into another DNS, thus forming the TNS, and finally, the decay of TNS into three fragments (Fig. 1).

The formation of an asymmetric DNS in the first stage of spontaneous ternary fission of ^{252}Cf takes place due to spontaneous clusterization of valence nucleons above the Pb core. Since the second and the third stages of spontaneous ternary fission take place in a nuclear time scale, the half-life time is determined in the first stage. This implies that spontaneous binary and ternary fission processes have very close half-lives within our model. Due to the Coulomb forces, the nuclei in TNS are collinearly placed, which approves the dominant role of the CCT process in spontaneous ternary fission. The yield ratio of ternary to binary fission is determined in the second stage; from the competition between the binary decay of symmetric DNS and TNS formation processes. A simple estimation of this ratio within our model gives the result 6.7×10^{-5}, which is close to the CCT yields observed in FOBOS experiments.

The presented model of spontaneous ternary fission describes well the experimentally observed features and quantities of spontaneous ternary fission of ^{252}Cf. New theoretical methods can be developed in the framework of the presented model for a more accurate quantitative description of the three stages of spontaneous ternary fission. The authors also hope for further increased interest among experimental scientists in the ternary fission phenomenon.

Declaration of competing interest

The authors declare that they have no known competing financial interests or personal relationships that could have appeared to influence the work reported in this paper.

Data availability

Data will be made available on request.

Acknowledgements

This work was initiated by the late Prof. V. V. Volkov and the authors are very grateful for his help, advice and valuable discussions.

The authors would like to thank Prof. G.G. Adamian, Prof. A.K. Nasirov and Dr. A. Rahmatinejad for their fruitful discussions during the progress of this work.

References

[1] G. Gamow, Nature (London) 122 (1928) 805.
[2] N. Bohr, J.A. Wheeler, Phys. Rev. 56 (1939) 426.
[3] R.D. Present, J.K. Knipp, Phys. Rev. 57 (1940) 751.
[4] T. San-Tsiang, H. Zah-Wei, R. Chastel, L. Vigneron, Phys. Rev. 71 (1947) 382.
[5] M.L. Muga, H.R. Bowman, S.G. Thompson, Phys. Rev. 121 (1961) 270.
[6] H. Diehl, W. Greiner, Nucl. Phys. A 229 (1974) 29.
[7] H.M.A. Radi, J.O. Rasmussen, R. Donangelo, L.F. Canto, L.F. Oliveira, Phys. Rev. C 26 (1982) 2049.
[8] O. Tanimura, T. Fliessbach, Z. Phys. A Hadrons Nucl. 328 (1987) 475.
[9] J.P. Theobald, P. Heeg, M. Mutterer, Nucl. Phys. A 502 (1989) 343.
[10] A. Sandulescu, A. Florescu, F. Carstoiu, W. Greiner, J. Phys. G, Nucl. Phys. 23 (1997) L7.
[11] Y.V. Pyatkov, D.V. Kamanin, A.A. Alexandrov, I.A. Alexandrova, S.V. Khlebnikov, S.V. Mitrofanov, V.V. Pashkevich, Y.E. Penionzhkevich, Y.V. Ryabov, E.A. Sokol, V.G. Tishchenko, A.N. Tjukavkin, A.V. Unzhakova, S.R. Yamaletdinov, Phys. At. Nucl. 66 (2003) 1631.
[12] Y.V. Pyatkov, D.V. Kamanin, W. von Oertzen, A.A. Alexandrov, I.A. Alexandrova, O.V. Falomkina, N.A. Kondratjev, Y.N. Kopatch, E.A. Kuznetsova, Y.E. Lavrova, A.N. Tyukavkin, W. Trzaska, V.E. Zhuhcko, Eur. Phys. J. A 45 (2010) 29.
[13] D.V. Kamanin, Y.V. Pyatkov, Clusterization in ternary fission, in: C. Beck (Ed.), Clusters in Nuclei, Volume 3, Springer International Publishing, Cham, 2014, pp. 183–246.
[14] Y.V. Pyatkov, D.V. Kamanin, A.A. Alexandrov, I.A. Alexandrova, E.A. Kuznetsova, Y.E. Lavrova, A.O. Strekalovsky, O.V. Strekalovsky, V.E. Zhuchko, Phys. Proc. 74 (2015) 67.
[15] Y.V. Pyatkov, D.V. Kamanin, A.A. Alexandrov, I.A. Alexandrova, Z.I. Goryainova, V. Malaza, N. Mkaza, E.A. Kuznetsova, A.O. Strekalovsky, O.V. Strekalovsky, V.E. Zhuchko, Phys. Rev. C 96 (2017) 064606, arXiv:1709.00170 [nucl-ex].
[16] A.K. Nasirov, W.V. Oertzen, R.B. Tashkhodjaev, Pramana 85 (2015) 367, arXiv:1411.4370 [nucl-th].
[17] K.R. Vijayaraghavan, V.G. Lakshmi, P. Prema, M. Balasubramaniam, J. Phys. G, Nucl. Phys. 46 (2019) 025103.
[18] W. von Oertzen, A.K. Nasirov, Eur. Phys. J. A 56 (2020) 299, arXiv:2007.02231 [nucl-th].
[19] A.V. Karpov, Phys. Rev. C 94 (2016) 064615.
[20] R.B. Tashkhodjaev, A.K. Nasirov, W. Scheid, Eur. Phys. J. A 47 (2011) 136, arXiv:1108.5461 [nucl-th].
[21] C. Kokila, M. Balasubramaniam, J. Phys. G, Nucl. Phys. 48 (2021) 025102.
[22] W. von Oertzen, A.K. Nasirov, R.B. Tashkhodjaev, Phys. Lett. B 746 (2015) 223.
[23] T.V. Chuvilskaya, Y.M. Tchuvil'sky, Phys. Rev. C 99 (2019) 024301.
[24] A.K. Nasirov, R.B. Tashkhodjaev, W. von Oertzen, Eur. Phys. J. A 52 (2016) 135.

[25] K.R. Vijayaraghavan, M. Balasubramaniam, W. von Oertzen, Phys. Rev. C 90 (2014) 024601.
[26] R.B. Tashkhodjaev, A.I. Muminov, A.K. Nasirov, W. von Oertzen, Y. Oh, Phys. Rev. C 91 (2015) 054612, arXiv:1503.03158 [nucl-th].
[27] P. Holmvall, U. Köster, A. Heinz, T. Nilsson, Phys. Rev. C 95 (2017) 014602, arXiv:1612.06583 [nucl-th].
[28] R.B. Tashkhodjaev, A.K. Nasirov, S.A. Kalandarov, O.K. Ganiev, Phys. Rev. C 107 (2023) 044611.
[29] J.B. Natowitz, H. Pais, G. Röpke, Phys. Rev. C 107 (2023) 014618, arXiv:2211.13492 [nucl-th].
[30] D.N. Poenaru, B. Dobrescu, W. Greiner, arXiv e-prints, nucl-th/0001046, 2000.
[31] R.B. Tashkhodjaev, A.K. Nasirov, E.K. Alpomeshev, Phys. Rev. C 94 (2016) 054614, arXiv:1610.04981 [nucl-th].
[32] V.V. Volkov, G.G. Adamian, N.V. Antonenko, E.A. Cherepanov, A.K. Nasirov, Nuovo Cimento A Ser. 110 (1997) 1127.
[33] G.G. Adamian, N.V. Antonenko, W. Scheid, Nucl. Phys. A 618 (1997) 176.
[34] A.K. Nasirov, G. Giardina, G. Mandaglio, M. Manganaro, F. Hanappe, S. Heinz, S. Hofmann, A.I. Muminov, W. Scheid, Phys. Rev. C 79 (2009) 024606, arXiv:0812.4410 [nucl-th].
[35] S.A. Kalandarov, G.G. Adamian, N.V. Antonenko, W. Scheid, Phys. Rev. C 82 (2010) 044603, arXiv:1003.3427 [nucl-th].
[36] I.S. Rogov, G.G. Adamian, N.V. Antonenko, Phys. Rev. C 100 (2019) 024606.
[37] I.S. Rogov, G.G. Adamian, N.V. Antonenko, Phys. Rev. C 104 (2021) 034618.
[38] I.S. Rogov, G.G. Adamian, N.V. Antonenko, Phys. Rev. C 105 (2022) 034619.
[39] V.V. Volkov, E.A. Cherepanov, S.A. Kalandarov, Phys. Part. Nucl. Lett. 13 (2016) 729.
[40] V.V. Volkov, S.A. Kalandarov, Phys. Part. Nucl. Lett. 13 (2016) 157.
[41] K.H. Schmidt, W. Morawek, Rep. Prog. Phys. 54 (1991) 949.
[42] A.B. Quint, W. Reisdorf, K.H. Schmidt, P. Armbruster, F.P. Heßberger, S. Hofmann, J. Keller, G. Münzenberg, H. Stelzer, H.G. Clerc, W. Morawek, C.C. Sahm, Z. Phys. A Hadrons Nucl. 346 (1993) 119.
[43] W. Greiner, J.Y. Park, W. Scheid, Nuclear Molecules, 1995.
[44] C. Beck, Clusters in Nuclei, vol. 1, Lecture Notes in Physics, vol. 818, 2010.
[45] C. Beck, Clusters in Nuclei, vol. 2, Lecture Notes in Physics, vol. 848, 2012.
[46] C. Beck, Clusters in Nuclei, vol. 3, Lecture Notes in Physics, vol. 875, 2014.
[47] G. Audi, A.H. Wapstra, C. Thibault, Nucl. Phys. A 729 (2003) 337.
[48] C.Y. Wong, Phys. Rev. Lett. 31 (1973) 766.
[49] A.B. Migdal, Theory of Finite Fermi Systems and Applications to Atomic Nuclei, Interscience Publishers, 1967, p. 319.
[50] S. Raman, C.H. Malarkey, W.T. Milner, C.W. Nestor Jr., P.H. Stelson, At. Data Nucl. Data Tables 36 (1987) 1.
[51] A. Nasirov, A. Fukushima, Y. Toyoshima, Y. Aritomo, A. Muminov, S. Kalandarov, R. Utamuratov, Nucl. Phys. A 759 (2005) 342.